

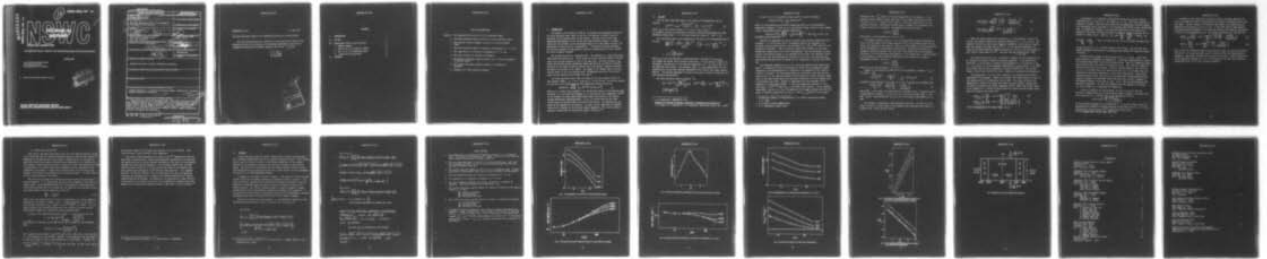
AD-A035 456

NAVAL SURFACE WEAPONS CENTER WHITE OAK LAB SILVER SP--ETC F/G 17/5  
THE NOISE EQUIVALENT POWER OF THE AMORPHOUS-GETE/SIOX TWO COLOR--ETC(U)  
JUN 76 K P SCHARNHORST, D L DEMSKE, G M BLACK  
NSWC/WOL/TR-76-98

UNCLASSIFIED

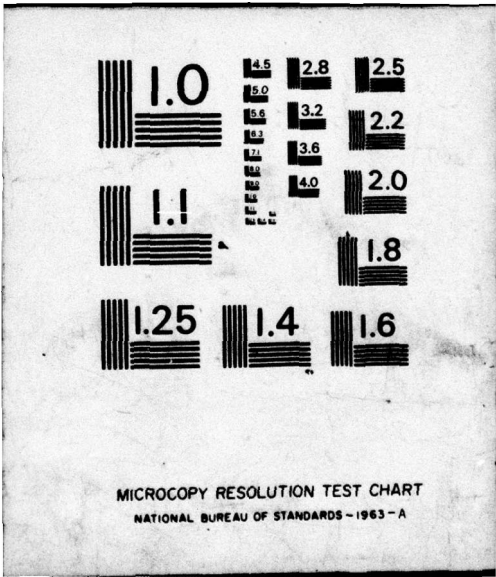
NL

| OF |  
AD  
A035456  
1



END

DATE  
FILMED  
3-77



ADA 035456

NSWC/WOL/TR 76-98

12

NSWC/WOL/TR 76-98

# NSWC

**TECHNICAL  
REPORT**

**WHITE OAK LABORATORY**

**THE NOISE EQUIVALENT POWER OF THE AMORPHOUS-GeTe/SiO<sub>x</sub> TWO COLOR DETECTOR**

18 JUNE 1976

NAVAL SURFACE WEAPONS CENTER  
WHITE OAK LABORATORY  
SILVER SPRING, MARYLAND 20910

● Approved for public release; distribution unlimited

D D C  
RECEIVED  
FEB 10 1977  
C

**NAVAL SURFACE WEAPONS CENTER  
WHITE OAK, SILVER SPRING, MARYLAND 20910**

UNCLASSIFIED

SECURITY CLASSIFICATION OF THIS PAGE (When Data Entered)

| REPORT DOCUMENTATION PAGE  |                       | READ INSTRUCTIONS<br>BEFORE COMPLETING FORM          |
|--|-----------------------|--|
| 1. REPORT NUMBER<br><b>14</b> NSWC/WOL/TR-76-98  | 2. GOVT ACCESSION NO. | 3. RECIPIENT'S CATALOG NUMBER                        |
| 4. TITLE (and Subtitle)<br><b>6</b> The Noise Equivalent Power of the Amorphous-GeTe/SiO <sub>x</sub> Two Color Detector.  |                       | 5. TYPE OF REPORT & PERIOD COVERED                   |
| 7. AUTHOR(s)<br><b>10</b> K. P./Scharnhorst<br>D. L./Demske<br>G. M./Black   |                       | 6. PERFORMING ORG. REPORT NUMBER                     |
| 9. PERFORMING ORGANIZATION NAME AND ADDRESS<br>Naval Surface Weapons Center<br>White Oak Laboratory<br>White Oak, Silver Spring, Maryland 20910  |                       | 8. CONTRACT OR GRANT NUMBER(s)                       |
| 10. PROGRAM ELEMENT, PROJECT, TASK AREA & WORK UNIT NUMBERS<br>62766N; 61112;  |                       | 9. Technical rept.                                   |
| 11. CONTROLLING OFFICE NAME AND ADDRESS<br><b>16</b> F61120  |                       | 10. ZF6112001 / WR0121                               |
| 12. MONITORING AGENCY NAME & ADDRESS (if different from Controlling Office)<br><b>13</b> 247.  |                       | 11. REPORT DATE<br>Jun 1976                          |
| 13. NUMBER OF PAGES<br>22  |                       | 12. SECURITY CLASS. (of this report)<br>UNCLASSIFIED |
| 14. DISTRIBUTION STATEMENT (of this Report)<br>Approved for public release; distribution unlimited   |                       | 13a. DECLASSIFICATION/DOWNGRADING SCHEDULE           |
| 15. DISTRIBUTION STATEMENT (of the abstract entered in Block 20, if different from Report)   |                       |  |
| 16. SUPPLEMENTARY NOTES  |                       |  |
| 17. KEY WORDS (Continue on reverse side if necessary and identify by block number)<br>Infrared Detection, 1-2 and 8-14 $\mu\text{m}$ Spectral Ranges, Responsivity, 1/f Noise, Thermal Response of a-GeTe/SiO <sub>x</sub> .   |                       |  |
| 18. ABSTRACT (Continue on reverse side if necessary and identify by block number)<br>Expressions for the noise equivalent power, NEP of the two color detector in both spectral regions, $\lambda = 1.0\text{-}2.0 \mu\text{m}$ and $\lambda = 8.0\text{-}14.0 \mu\text{m}$ are derived. Experimental results for the NEPs are presented. The best room temperature NEPs to date at $\lambda = 1.1 \mu\text{m}$ and at $\lambda = 8.0$ to $11.5 \mu\text{m}$ are about $10^{-8}$ watts/(Hz) <sup>1/2</sup> between 5 and 10 Hz for a 10 by 10 mil detector element. Means of improving detector performance are discussed. |                       |  |

DD FORM 1 JAN 73 1473

EDITION OF 1 NOV 66 IS OBSOLETE  
S/N 0102-014-6601

UNCLASSIFIED

SECURITY CLASSIFICATION OF THIS PAGE (When Data Entered)

391 596

mt

NSWC/WOL/TR 76-98

18 June 1976

The Noise Equivalent Power of the Amorphous-GeTe/SiO<sub>x</sub> Two Color Detector.

The work reported herein was carried out in the Solid State Branch of the Materials Division of the Research and Technology Department as part of the Independent Exploratory Development Program; IED Task No. ZF61112001

*J R Dixon*  
J. R. DIXON  
By direction

|                                    |                                     |
|------------------------------------|-------------------------------------|
| White Section                      | <input checked="" type="checkbox"/> |
| Red Section                        | <input type="checkbox"/>            |
| BY DISTRIBUTION/AVAILABILITY CODES |                                     |
| Dist.                              | AVAIL. and/or SPECIAL               |
| A                                  |                                     |

CONTENTS

|      |  |    |
|------|--|----|
| I.   | INTRODUCTION                                     | 4  |
| II.  | The NEP  | 5  |
| III. | Experimental Results and Discussion              | 11 |
|      | 1. General Remarks.                              | 11 |
|      | 2. The 8.0 to 11.5 $\mu\text{m}$ Spectral Range. | 11 |
|      | 3. The 1.0 to 2.0 $\mu\text{m}$ Spectral Range.  | 11 |
|      | 4. Current Noise and the NEP.                    | 13 |
| IV.  | APPENDIX   | 15 |

LIST OF ILLUSTRATIONS

- Figure 1 - The responsivity in the 8.0 to 11.5  $\mu\text{m}$  spectral range.
- 2 - The noise equivalent power in the 8.0 to 11.5  $\mu\text{m}$  spectral range.
  - 3 - The relative spectral response in the 6.5 to 13.5  $\mu\text{m}$  spectral range.
  - 4 - The noise equivalent power as a function of frequency at  $\lambda = 1.1 \mu\text{m}$ .
  - 5 - The responsivity as a function of frequency at  $\lambda = 1.1 \mu\text{m}$ .
  - 6 - The noise voltage as a function of frequency.
  - 7 - The current noise power spectral density at  $f = 10 \text{ Hz}$  as a function of applied current.
  - 8 - The current noise power spectral density as a function of frequency.
  - 9 - Schematic of a heat conduction problem.

## I. INTRODUCTION

The purpose of this report is twofold. We present our experimental results on the noise equivalent power (NEP) of the two color detector in order to give an indication of the present status of this device. Secondly, based on our room temperature measurements of the current noise power spectral density, we derive expressions for the NEPs in both wavelength bands and use these NEPs to predict the performance of future detector configurations. The general operating principles and the gross features of some possible practical implementations of this detector are given in Patent #3743995.

The detector material is amorphous GeTe. The substrate is a  $\text{SiO}_x$  based glass ribbon about 40 microns thick. Silver paint was used to bond the ribbon to the substrate (Al) and the substrate in turn to the heat sink. The front surface of the ribbon and the back surface immediately behind the detector, as well as a certain perimeter of the ribbon around the detector were left exposed. Thermal relaxation took place in the plane of the ribbon. The length of the thermal path to the heat sink was about 1.5 mm in the present work. The detector area was a 10 by 10 mil. square and the detector film thickness was 1600 Å.

The noise equivalent power, NEP, was chosen as the basic figure of merit in both spectral ranges;  $\lambda = 1.0$  to  $2.0 \mu\text{m}$  and  $\lambda = 7.0$  to  $13.0 \mu\text{m}$ . In the next section we show that at low frequencies the room temperature NEP may be written:

$$\text{NEP}(300^\circ\text{K}) = \sqrt{\frac{C_2 A}{df}} \left\{ \sigma_0 \langle H^2 \rangle^{1/2} / \langle \Delta\sigma^2(f,A) \rangle^{1/2} \right\} \quad (1)$$

where  $C_2$  is a current noise constant,  $A$  is the detector area,  $d$  is the detector film thickness,  $f$  is the operating frequency,  $\sigma_0$  is the detector dark conductance,  $\langle H^2 \rangle^{1/2}$  is the incident root mean square (RMS) power density and  $\Delta\sigma(f,A)$  is the spatial average differential photoconductance. In Eq. (1) we have used the fact that current noise is the major source of noise in this device. The equation sets the stage for our approach to the analysis. In order to fully appreciate its implications we will consider the two spectral ranges separately. For a given detector material we mainly have to discuss the quantity  $\langle \Delta\sigma^2(f,A) \rangle^{1/2}$ .

## II. The NEP.

The root mean square RMS signal at the input of the preamplifier may be written:

$$\langle V_s^2 \rangle^{1/2} = I_{DC} R' \frac{\langle \Delta \sigma^2(f, A) \rangle^{1/2}}{\sigma_0} \left[ 1 + (\omega C' R')^2 \right]^{1/2} \quad (2)$$

where  $I_{DC}$  is the DC drive current,  $R' = [1/R_L + 1/R_S + 1/R_0]^{-1}$ ;  $R_L$ ,  $R_S$  and  $R_0$  are the load resistance, detector resistance and preamplifier input resistance respectively.  $C'$  is the shunt capacitance across  $R'$ , and  $\omega = 2\pi f$ .

The total noise power in unit bandwidth at the input of the preamplifier may be written;

$$\frac{\langle V_{TN}^2 \rangle^{1/2}}{(\Delta f)^{1/2}} = \left[ \frac{\langle V_{CN}^2 \rangle + \langle V_{JN}^2 \rangle}{(\Delta f)^{1/2}} \right]^{1/2} = \left[ \frac{C_2}{Vf} + (N.F.)^2 \frac{4KT}{I_{DC}^2 R} \right]^{1/2} \quad (3)$$

$$\times \frac{R' I_{DC}}{[1 + (\omega C' R')^2]^{1/2}}$$

where  $V_{TN}$  is the total RMS noise voltage measured in bandwidth  $\Delta f$  and  $V_{CN}$ ,  $V_{JN}$  are current and thermal noise voltages respectively,  $V$  is the detector volume,  $K$  is Boltzmann's constant and  $T$  is the absolute temperature,  $R^{-1} = R_L^{-1} + R_S^{-1}$  and  $(N.F.)$  is the amplifier noise figure. The expression  $I_{DC}^2/f$  is a good approximation for the observed drive current and frequency dependence of the current noise power spectral density.<sup>1</sup> The inverse dependence of current noise power on detector volume has also been verified experimentally.

The noise equivalent power is defined<sup>2</sup> as:

$$NEP \equiv \langle H^2 \rangle^{1/2} A \frac{\langle V_{TN}^2 \rangle^{1/2}}{(\Delta f)^{1/2} \langle V_S^2 \rangle^{1/2}} = \langle H^2 \rangle^{1/2} A \left[ \frac{C_2}{Vf} + (N.F.)^2 \frac{4KT}{I_{DC}^2 R} \right]^{1/2} \quad (4)$$

$$\left[ \frac{\langle \Delta \sigma^2(f, A) \rangle^{1/2}}{\sigma_0} \right]$$

<sup>1</sup> K. P. Scharnhorst, NSWC/WOL/TR 76-97.

<sup>2</sup> Elements of Infrared Technology, Generation, Transmission and Detection, P. W. Kruse, L. D. McGlauchlin, R. B. McQuistan, (John Wiley & Sons, Inc., 1962).

In the 8.0 to 11.5  $\mu\text{m}$  spectral range,  $\Delta\sigma(f,A)$  is purely bolometric:

$$\langle \Delta\sigma^2(f,A) \rangle^{1/2} / \sigma_0 = \frac{E}{KT^2} \langle \Delta T^2(f,A) \rangle^{1/2}$$

where  $E$  is the conductivity activation energy and  $\Delta T(f,A)$  is the differential temperature response.<sup>3</sup> In the 1.0 to 2.0  $\mu\text{m}$  spectral range,  $\Delta\sigma(f,A)$  is more complex. It has a photoconductive and a thermal component:

$$\langle \Delta\sigma^2(f,A) \rangle^{1/2} / \sigma_0 = \left( \left( \frac{\Delta\sigma_{pc}}{\sigma_0} + \frac{E}{KT^2} \Delta T(f,A) \right)^2 \right)^{1/2}, \text{ where } \Delta\sigma_{pc} \text{ is the } \quad (5)$$

fundamental photoconductance.

Consider the dependence of  $\Delta\sigma(f,A)$  on detector and substrate dimensions and on frequency. It is well known that if interference effects are neglected,  $\Delta\sigma_{pc}$  increases with decreasing detector film thickness;<sup>3</sup>  $\Delta\sigma_{pc} \propto \frac{H}{d} (1 - e^{-\alpha d})$  where  $\alpha$  is the absorption coefficient. When interference effects are included, the situation becomes more complicated but one finds experimentally that the absorptance is maximized in both spectral ranges if the amorphous film is only a few thousand  $\text{\AA}$  thick.<sup>4</sup> We also note that the photoconductive response is very fast, with submicrosecond time constant and hence does not depend on  $f$  at frequencies of interest here ( $f \leq 200$  Hz).

The bolometric response at 8.0 to 11.5  $\mu\text{m}$  was discussed in great detail elsewhere.<sup>5</sup> An extension of these calculations to a model which includes the thermal properties of the bonding material is indicated in the appendix of this report as a matter of interest. For the present purpose we only need to know that the response is slow; of the order of hundreds of milliseconds for lateral substrate dimensions of the order of millimeters and substrate thicknesses as in the example given in the present work (40 $\mu$ ). Suppose we approximate the time dependence of the response by a single time constant,  $\tau$ . Then the temperature response is of the form  $\Delta T_{st} [1 + (\omega\tau)^2]^{-1/2}$  where  $\Delta T_{st}$  is the steady state response. In the frequency range above a few Hz, e.g. 5 Hz, the amplitude of the signal received from the bolometer is therefore proportional to  $\Delta T_{st} / \tau f$ . Now  $\Delta T_{st} \propto \frac{1}{\bar{K}}$  where  $\bar{K}$  is the thermal

<sup>3</sup> Photoelectric Effects in Semiconductors, S. M. Ryvkin (Consultants Bureau, N. Y., 1964)

<sup>4</sup> H. R. Riedl, private communication.

<sup>5</sup> K. P. Scharnhorst, NOLTR 72-184.

conductance and  $\tau = \frac{\bar{C}}{\bar{K}}$  where  $\bar{C}$  is the heat capacitance of the bolometer. If we picture a square detector element with area  $\ell^2$  and a square substrate with area  $L^2 \equiv (\gamma\ell)^2$ , i.e.  $\gamma > 1$ , then  $\bar{C} = CDL^2$ , where  $C$  is the heat capacity and  $D$  is the substrate thickness. The detector thermal mass is assumed to be negligible with respect to that of the substrate. The temperature response becomes:

$$\Delta T(f,A) \propto \frac{B_2(d)H}{2\pi DL^2 Cf}$$

where  $B_2(d)$  is the absorptance at 8.0 to 11.5  $\mu\text{m}$ .

The thermal response in the 1.0 to 2.0  $\mu\text{m}$  range differs somewhat from that at 8.0 to 11.5  $\mu\text{m}$  because in the former range the film is the absorber whereas in the latter the substrate is the absorber. Hence the film thickness enters the expression for the absorptance in a different functional form. We need not calculate this dependence explicitly however, since the size of the effect for film thicknesses of interest to us was determined experimentally in the present work. Rough estimates of the response for other substrate dimensions may be obtained by scaling our experimental results. We write:

$$\Delta T(f,A) \propto \frac{B_1(d)H}{2\pi DL^2 Cf}$$

where  $B_1(d)$  is the absorptance at 1.0 to 2.0  $\mu\text{m}$ .

Suppose we are detecting the RMS value of the fundamental component,  $\langle \rangle_F$  of the signal. Then:

$$\frac{\langle \Delta\sigma^2(f,A) \rangle_F^{1/2}}{\sigma_o} = \frac{\langle \Delta\sigma_{pc}^2 \rangle_F^{1/2}}{\sigma_o} + \frac{E}{KT^2} \langle \Delta T^2(f,A) \rangle_F^{1/2} \quad (6)$$

According to what has been said so far we can write for square wave chopped light:

$$\frac{\langle \Delta\sigma^2(f,A) \rangle_F^{1/2}}{\sigma_o} = \sqrt{\frac{2}{\pi}} \left[ \frac{\Delta\sigma_{pc}^{st}}{\sigma_o} + \frac{B(d)H_o E}{2\pi DL^2 CfKT^2} \right] \quad (7)$$

where  $\Delta\sigma_{pc}^{st}$  is the steady state photoconductive response and  $H_o$  is the peak to peak incident radiant intensity. In the 8.0 to 11.5  $\mu\text{m}$  spectral range,  $\Delta\sigma_{pc}^{st} = 0$  and  $B(d) \equiv B_2(d)$ . Substituting back into Eq. (4) yields explicit expressions for the NEPs.

We are mainly interested in room temperature operation. At 300°K it is possible to choose  $I_{DC}$  large enough to make thermal noise negligible with respect to current noise. Hence the NEPs become:

$$\text{NEP (300°K)}_{\lambda = 1-2\mu} = H_0 \sqrt{\frac{C_2 A'}{df}} \left[ \frac{\Delta\sigma_{pc}^{st}}{\sigma_0} + \frac{H_0 B_1(d)E}{2\pi f C D A \gamma^2 K T^2} \right]^{-1} \quad (8)$$

$$\text{NEP (300°K)}_{\lambda = 8-11.5\mu} = \sqrt{\frac{C_2}{df}} A^{3/2} D \left[ \frac{B_2(d)E}{2\pi f C \gamma^2 K T^2} \right]^{-1} \quad (9)$$

There are several points worth noting here. As the substrate volume is decreased, the thermal response will eventually dominate at  $\lambda = 1.0$  to  $2.0 \mu\text{m}$ . The response of the device will become completely bolometric in both spectral regions. When this happens, both NEPs vary as  $A^{3/2} D$ . If the substrate dimensions are large and the photoconductive response dominates at  $1.0$  to  $2.0 \mu\text{m}$ , then the NEP in that spectral range varies as  $A^{1/2}$ . Also note that NEP (300°K) varies as  $\sqrt{f}$ .

$\lambda = 8-11.5\mu\text{m}$

The question now arises if it is possible to improve two color operation e.g. by cooling or by making a change in some other parameter. As was pointed out previously,  $d$  can be chosen to optimize the absorptance at  $1.6 \mu\text{m}$  and at  $9.5 \mu\text{m}$ , i.e.  $\Delta\sigma_{pc}$  and  $B_2(d)$  can be maximized simultaneously. A good choice is  $d \approx 2000 \text{ \AA}$ . We also note that  $1/f$  noise contributes a factor of  $\sqrt{1/d}$  in Eqs. (8) and (9). Because of this factor the NEP will have a tendency to increase with decreasing  $d$ .

The temperature is the only other parameter to be considered for possible improvements of performance. Before we can assess this effect however, we have to add thermal noise in the expressions for the NEPs. The reason is that as the temperature is lowered, the sample resistance increases rapidly, current flow decreases and thermal noise becomes comparable with or larger than current noise. As the temperature is lowered the photoconductive response quickly becomes larger than the bolometric one and we have:

$$\text{NEP (T)}_{\lambda=1-2\mu} = H_0 A \left[ \frac{C_2}{Vf} + (\text{N.F.})^2 \frac{4KT}{I_{DC}^2 R} \right]^{1/2} \frac{\Delta\sigma_{pc}^{st} R_s}{\sigma_0} \quad (10)$$

$$\text{NEP (T)}_{\lambda=8-11.5\mu} = A^2 D \left[ \frac{C_2}{Vf} + (\text{N.F.})^2 \frac{4KT}{I_{DC}^2 R} \right]^{1/2} \left[ \frac{B_2(d)E}{2\pi f C \gamma^2 K T^2} \right] \quad (11)$$

\* K. P. Scharnhorst, H. R. Riedl, NOLTR 72-196.

In principle it is necessary to distinguish between two possible loading conditions now;  $R_L \ll R_S$  or  $R_L =$  very large e.g.  $R_L \approx R_S$ . The latter condition is unrealistic, however, since the noise figure of the preamplifier increases rapidly with increasing circuit resistance at the extremely high ( $>10^9 \Omega$ ) values contemplated here. An additional drawback is the increased sensitivity of the circuit to mechanical vibrations, although with modern integrated circuit technology this is perhaps of lesser concern. When  $R_L \ll R_S$ , then  $\frac{4KT}{I_{DC}^2 R} = \frac{4KTR_S}{V_o^2 R_L}$ ; when  $R_L = R_S$  then  $\frac{4KT}{I_{DC}^2 R} = \frac{8KTR_S}{V_o^2}$ . Hence in either case the 1.0 to 2.0  $\mu\text{m}$  NEP decreases with

cooling and the 8.0 to 11.5  $\mu\text{m}$  NEP increases with cooling. Only the short wavelength, fundamental photoconductive performance may therefore be improved by means of cooling.

We have tacitly assumed in this discussion that  $C_2$ , the bulk current noise power constant is independent of temperature. It has been suggested<sup>7</sup> that  $C_2$  should be inversely proportional to the free carrier density. Hence its temperature dependence would be that of  $R_S$  which is exponential in  $1/T$ . This would not change the essential conclusions just reached, as may be verified from Eqs. (10) and (11); the 1.0 to 2.0  $\mu\text{m}$  NEP would still decrease and the 8.0 to 11.5  $\mu\text{m}$  NEP would still increase with decreasing temperature, in fact faster than before. Some further reflections based on Eqs. (10) and (11) also reveal that the photoconductive NEP begins to increase at temperatures below 200°K where  $\Delta\sigma_{pc}$  reaches a maximum if the loading condition is such that  $R_L \ll R_S$ . If  $R_L \approx R_S$ , the photoconductive NEP continues to decrease. The last two statements are true regardless of whether  $C_2 \propto R_S$  or whether  $C_2$  is independent of temperature.

It may be worthwhile to draw attention once more to the fact that the relatively strong sensitivity of the bolometric NEPs to changes in substrate area only holds when  $\omega\tau > 1$ . The RMS value of the fundamental of  $\Delta T$  is:

$$\langle \Delta T^2(f, A) \rangle_F^{1/2} = \frac{\sqrt{2}}{\pi} \frac{B(d)\Delta T_{st} H_o}{[1 + (\omega\tau)^2]^{1/2}}$$

As the substrate dimensions are decreased and  $\tau \rightarrow 0$ , or in any case at very low frequencies the bolometric response saturates and the NEPs, both at 1.0 to 2.0  $\mu\text{m}$  and at 8.0 to 11.5  $\mu\text{m}$ , vary as  $A^{1/2}$  (neglecting thermal noise).

<sup>7</sup> F. N. Hooge, Phys. Letters, A29, 139 (1969).

In summary we have found that cooling the detector decreases (improves) the 1.0 to 2.0  $\mu\text{m}$  NEP and causes the photoconductive response to dominate in this spectral range. Cooling increases the bolometric NEP however, thus diminishing the usefulness of the device at 8.0 to 11.5  $\mu\text{m}$ . On the other hand we found earlier that decreasing the dimensions of the substrate enhances the bolometric performance in favor of the photoconductive one. The complete expressions for the NEPs are:

$$\text{NEP(T)}_{\lambda = 1-2\mu} = H_o \left[ \frac{C_2 A}{df} + (\text{N.F.})^2 \frac{4KTA^2}{I_{DC}^2 R} \right]^{1/2} / \left[ \frac{\Delta\sigma_{pc}^{st}}{\sigma_o} + \frac{B_1(d)EH_o}{2\pi fCDA\gamma^2 KT^2} \right] \quad (12)$$

$$\text{NEP(T)}_{\lambda = 8 - 11.5\mu} = \left[ \frac{C_2 A}{df} + (\text{N.F.})^2 \frac{4KTA^2}{I_{DC}^2 R} \right]^{1/2} / \left[ \frac{B_2(d)E}{2\pi fCDA\gamma^2 KT^2} \right] \quad (13)$$

Thus in order to decrease the NEPs in both spectral ranges one simply miniaturizes the device. If it were desirable finally to bring out the fast photoconductive response to some extent one would have to resort to cooling. Complete suppression of the bolometric response at 1.0 to 2.0  $\mu\text{m}$  without at the same time producing a useless NEP at 8.0 to 11.5  $\mu\text{m}$  is however impossible.

### III. EXPERIMENTAL RESULTS AND DISCUSSION

#### 1) General Remarks.

In addition to the particular detector configuration under discussion in the present work, several other structures were explored and discarded because they yielded lower responsivities. Thus thicker glass substrates or direct bonding to the heat sink which yields a short thermal path perpendicular to the plane of the detector gave considerably reduced responsivities. On the other hand changing bonding material from silver paint to epoxy or changing the "heat sink" from aluminum to fiber glass had no significant effect on the responsivity. The best results were obtained with the construction and mounting procedures reported in this work.

We also found that ambients had a strong effect on the detector resistance and that an overlay of  $\text{SiO}_x$  stabilized this resistance.<sup>1</sup> The performance of passivated detectors has not been evaluated however.

#### 2) The 8.0 to 11.5 $\mu\text{m}$ Spectral Range.

In this spectral range the responsivity should be proportional to  $1/f$  at frequencies of interest here. This is roughly what we find, Figure 1. The NEP on the other hand should increase with frequency as  $\sqrt{f}$ , Figure 2, Eq. (9). Again this is roughly what we find. The increase of the NEP at high frequencies with decreasing bias voltage is due to a decrease in the corner frequency for current noise with decreasing bias current; at the higher frequencies and at low bias levels, thermal noise predominates.

The spectral response of a detector on ribbon glass in the 7.0 to 13.0  $\mu\text{m}$  window is shown in Figure 3.

#### 3) The 1.0 to 2.0 $\mu\text{m}$ Spectral Range.

In this part of the spectrum the detectors exhibit two very different speeds of response. There is the fast fundamental photoconductive response and in addition to this there is also the slow bolometric response. It is believed that the slow response is due to the energy transferred to the lattice as photoexcited carriers recombine. This is therefore an internal thermal effect as distinguished from the induced thermal effect in the 8.0 to 11.5  $\mu\text{m}$  spectral range. It is known that the slow component can be attenuated very substantially by simply putting the amorphous films on sapphire rather than glass substrates. In this way it is possible to

measure the fundamental response. But as far as the two color detector is concerned, the slow response will always be present in the 1.0 to 2.0  $\mu\text{m}$  spectral range because low conductance  $\text{SiO}_x$ -glass substrates are needed for the bolometric response at 9.5  $\mu\text{m}$ .

As was pointed out in the previous section, the fast response has a submicro-second time constant. Hence the corresponding responsivity is not a function of frequency at low frequencies; certainly not in the range below a few hundred Hz, which is of primary interest to us. The NEP for this part of the response therefore varies as  $1/\sqrt{f}$ , Eq. (8). Because of the added slow response however, this  $1/\sqrt{f}$  behavior is not observed, Figure 4. We find instead that the NEP remains roughly constant between 5 and 100 Hz. Figure 5 shows the responsivity at  $\lambda = 1.1 \mu\text{m}$  as a function of frequency. It is indeed a strongly decreasing function of frequency below about 100 Hz, as expected from the superposition of fast and slow components. At low frequencies the slow component is seen to be of overriding importance. At high frequencies ( $f > 200 \text{ Hz}$ ) only the fast component remains.

At the higher frequencies,  $1/f$  noise runs into thermal noise and the NEP has a tendency to become truly independent of frequency. The improvement of the NEP at high bias voltages in this frequency range is of course due to the increasing corner frequency for current noise with increasing bias level.

The NEP throughout the entire 1.0 to 2.0  $\mu\text{m}$  spectral range may in first approximation be obtained from published data on the relative photoconductive spectral response for films on glass substrates,<sup>8</sup> assuming that the relative contributions of fast and slow components do not depend strongly on wavelength. Between  $\lambda = 1.1 \mu$  and  $\lambda = 1.6 \mu\text{m}$  the response decreases by a factor of three. This result was obtained by means of thick films in which interference effects were negligible. Films which are of interest for detector applications are relatively thin for several reasons; the thermal mass of the film should be small for maximum response at  $\lambda = 9.5 \mu\text{m}$  and, as mentioned above, the absorbance at 9.5  $\mu\text{m}$  happens to be largest for thin films. By placing the interference maximum for absorbance properly, i.e. by choosing the right film thickness, the drop in response at  $\lambda = 1.6 \mu\text{m}$  may probably be compensated to some extent.

---

<sup>8</sup> H. R. Riedl, K. P. Scharnhorst and D. G. Simons, *Infrared Physics*, 14, 139 (1974).

## 4) Current Noise and the NEP.

When work on this particular phase of the two color detector project started, it was clear that the only essential remaining question concerned the origins and magnitude of the current noise of the device. Responsivities in both spectral bands had already been studied extensively both experimentally and theoretically. With respect to noise however not even its origin was known with certainty let alone its magnitude, drive current and spectral dependence and its dependence on the dimensions of the sample. A major effort therefore went into clearing up this problem. The details of our findings were presented elsewhere.<sup>1</sup> In this section we give a brief account of the results.

The total noise voltage of the particular detector under discussion here is shown in Figure 6. It is evident that the major noise component in this device is current noise. We established however that it was possible to make practically noise free electrodes and we also found that the remaining bulk generated current noise power density could be expressed in the form:

$$\frac{\langle i^2 \rangle}{\Delta f} = C_o I_{DC}^\alpha / f^\beta \quad (14)$$

where  $\beta$  and  $\alpha$  are constants near 1.0 and 2.0 respectively over certain ranges of frequencies and currents, Figures 7 and 8. We established that  $C_o$  was equal to  $C_2/V$  and that the value of  $C_2$  is about  $2.4 \times 10^{-20} \text{ cm}^3 \text{ Hz}^{\beta-1}$  in a-GeTe. It is of course precisely this detailed evaluation of the current noise power spectral density which enabled us to analyze the noise equivalent power.

In terms of the "Microvolts-per-Volt" Index<sup>9</sup>,  $y$ , for resistors we have:

$$Y = 20 \log_{10} \left\{ 10^{12} \int_{\text{decade}} \frac{V_{cn}^2 (\mu V) df}{[I_{DC} R_S]^2} \right\}$$

where  $V_{cn}^2$  ( $\mu V$ ) is the open circuit RMS current noise voltage per unit bandwidth. Hence:

$$Y(\text{a-GeTe}) = 10 \log_{10} \left[ \frac{5.53 \times 10^{-8}}{dA(\text{cm}^3)} \right]$$

For a square resistor element, 1  $\mu\text{m}$  thick and 10 mils (250  $\mu\text{m}$ ) on a side, one has  $y = -0.53 \text{ db/decade}$  or  $0.94 \mu\text{V}/(\text{Volt decade})$ . If the dimensions are increased to 2.5 mm on the edge, we find  $y = -20.53 \text{ db/decade}$  or  $0.094 \mu\text{V}/(\text{Volt decade})$ . The

<sup>9</sup> G. T. Conrad Jr., N. Newman, A. P. Stansbury, IRE Trans. on Comp. Parts, CP-7, 1 (1960).

noise figure (index) for the large-area resistor is in fact excellent. These resistors have a value of 30 M $\Omega$  at room temperature.

The inverse volume dependence of  $C_0$  leads to the  $A^{3/2}$ -dependence of the bolometric NEP on detector area. Knowing the dimensional dependences of the NEPs and the results for the 10 x 10 mil detector discussed in this report we can establish the NEPs for other detector dimensions. Such estimates should start with NEPs which are about a factor of 1.7 lower than the ones shown in the Figures since some contact noise was present in the detectors discussed here. It is apparent from Eqs. (8) and (9), Section I that if sufficiently thin and self supporting substrates are produced and if in addition the detector dimensions are reduced, improved NEPs may be obtained. An elegant way of achieving this volume reduction of the detector is of course via the use of an evaporated or thermally grown  $\text{SiO}_x$  membrane on a crystalline Si-substrate-frame, as described in detail elsewhere.<sup>10</sup>

---

<sup>10</sup> Patent Disclosure #NC 60425, R. F. Greene and K. P. Scharnhorst

IV. APPENDIX

In this section we quote the Green's function for a certain two dimensional heat conduction problem more or less as a matter of general interest. This function may be used to estimate the effect of the thermal conductance of the bonding material on the bolometric response of the two color detector in both spectral ranges. The solution to this problem was not actually applied, however, because the bonding material was expected to have only a minor influence on the performance characteristics of this particular detector.

A schematic of the model is shown in Figure 9. Our method of solution follows closely that given in standard textbooks on conduction of heat in solids.<sup>11</sup> One takes the Laplace transform of the relevant heat conduction equations, solves the equations in transform space and takes the inverse transform to arrive at the Green's function. The inverse transform leads to a contour integral in complex transform space and to the problem of finding the residues of the integrand. In the present case the residues are related to the roots of a transcendental equation. The equation may easily be solved with the aid of an electronic computer.

The Green's function for this problem, i.e. the temperature response to unit instantaneous point sources at time  $t = 0$  and at  $(x,y) = (\pm x_0, y_0)$  is:

$$a \leq x \leq A$$

$$G(x,y,t) = \sum_{n=0}^{\infty} \sum_{m=0}^{\infty} \frac{\epsilon_n}{b} \cos(q_n y) \cos(q_n y_0) \exp[-tK_1(\beta_{mn}^2 + q_n^2)]$$

$$\left\{ \frac{i \cos[\beta_{mn} x_0] \sin[(A-x)K_0 \sqrt{\beta_{mn}^2 + q_n^2 (1 - K_2/K_1)}]}{\frac{d}{dp} D \Big|_{p = -K_1[\beta_{mn}^2 + q_n^2]}} \right\};$$

$$i \equiv \sqrt{-1}.$$

<sup>11</sup> Conduction of Heat in Solids, H. S. Carslaw and J. C. Jaeger (Oxford at the Clarendon Press, 1959).

$$x_0 \leq x \leq a$$

$$G(x, y, t) = \sum_{n=0}^{\infty} \sum_{m=0}^{\infty} \frac{\epsilon_n}{b} \cos(q_n y) \cos(q_n y_0) \exp[-t K_1 (\beta_{mn}^2 + q_n^2)]$$

$$\left\{ -\cos(\beta_{mn} x_0) [K_2 K_0 \sqrt{\beta_{mn}^2 + q_n^2 (1 - K_2/K_1)} \cos(K_0 \Delta \sqrt{\beta_{mn}^2 + q_n^2 (1 - K_2/K_1)}) \right.$$

$$\sin(\beta_{mn} (A-x)) + K_1 \beta_{mn} \sin(K_0 \Delta \sqrt{\beta_{mn}^2 + q_n^2 (1 - K_2/K_1)})$$

$$\left. \cos(\beta_{mn} (A-x)) \right] / K_1 \beta_{mn} i \frac{dD}{dp} \Big|_{p=-K_1 [\beta_{mn}^2 + q_n^2]} \left. \right\}$$

$$0 \leq x \leq x_0$$

$$G(x, y, t) = \sum_{n=0}^{\infty} \sum_{m=0}^{\infty} \frac{\epsilon_n}{b} \cos(q_n y) \cos(q_n y_0) \exp[-t K_1 (\beta_{mn}^2 + q_n^2)]$$

$$\left\{ \text{same as for } x_0 < x < a, \text{ except } x \leftrightarrow x_0 \right\}$$

The following definitions of symbols were used:

$$D(p) = [K_2 Q_{2n} \cosh(\Delta Q_{2n}) \cosh(a Q_{1n}) + K_1 \sinh(\Delta Q_{2n}) \sinh(a Q_{1n})], \text{ where } Q_{1n} \equiv \sqrt{p/K_1 + q_n^2}$$

$$Q_{2n} \equiv \sqrt{p/K_2 + q_n^2}, \quad K_{1,2} \equiv K_{1,2}/\rho c, \quad \Delta \equiv (A-a)$$

$$\text{and } q_n \equiv (n\pi/b).$$

The roots  $\beta_{mn}$  are determined by the equation:

$$[K_0 \beta_{mn} / \sqrt{\beta_{mn}^2 + q_n^2 (1 - K_2/K_1)}] \tan(\Delta K_0 \sqrt{\beta_{mn}^2 + q_n^2 (1 - K_2/K_1)})$$

$$\tan(\beta_{mn} a) = 1, \text{ with } K_0 \equiv \sqrt{K_1/K_2} \text{ and}$$

$$K_2 \leq K_1.$$

## FIGURE CAPTIONS

1. The responsivity as a function of frequency in the 8.0 to 11.5  $\mu\text{m}$  spectral range. The source was a blackbody at  $T = 500^\circ\text{K}$ . An 8.0 to 11.5  $\mu\text{m}$  filter was used to define the spectrum of incident radiation.
2. The noise equivalent power in the 8.0 to 11.5  $\mu\text{m}$  spectral range. The source was a blackbody at  $500^\circ\text{K}$ . An 8.0 to 11.5  $\mu\text{m}$  filter was used to define the spectrum of incident radiation.
3. The relative spectral response in the 6.5 to 13.5  $\mu\text{m}$  spectral range. A Perkin Elmer Model 12B spectrometer with a NaCl prism was used for this measurement.
4. The noise equivalent power as a function of frequency at  $\lambda = 1.1 \mu\text{m}$ .
5. The responsivity as a function of frequency at  $\lambda = 1.1 \mu\text{m}$ .
6. The noise voltage at different bias levels,  $V(\text{Volts})$ , as a function of frequency. The load resistance was  $2.6 \text{ M}\Omega$  and  $R_L \ll R_S$ .
7. The current noise power spectral density of a-GeTe as a function of the applied current at  $f = 10\text{Hz}$ .
  - - Chromium electrodes
  - ◇ - Gold electrodes
  - - Molybdenum electrodes
8. The current noise power spectral density of a-GeTe as a function of frequency.
  - - Chromium Electrodes
  - ◇ - Gold electrodes
  - - Molybdenum electrodes
9. A schematic of the two dimensional heat conduction problem considered in the appendix. Thermal conductivities, specific heats and densities are indicated by  $K_{1,2}$ ,  $C_{1,2}$  and  $\rho_{1,2}$  respectively. The solution given in the present work assumes  $\rho_1 C_1 = \rho_2 C_2$ . Two unit instantaneous point sources at  $t = 0$  are located symmetrically at  $(x,y) = (\pm x_0, y_0)$ . Boundary conditions are as shown next to the arrows.

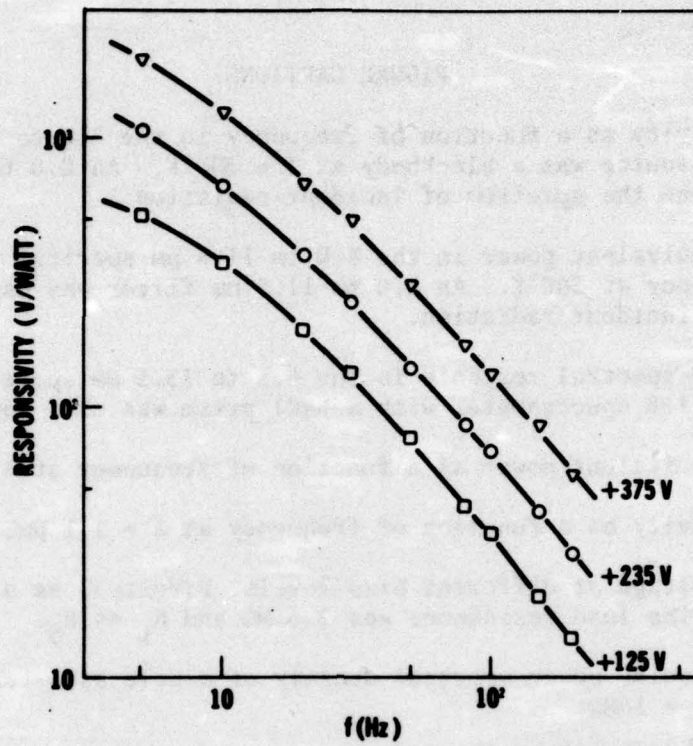


FIG. 1 THE RESPONSIVITY IN THE 8.0 TO 11.5 μm SPECTRAL RANGE

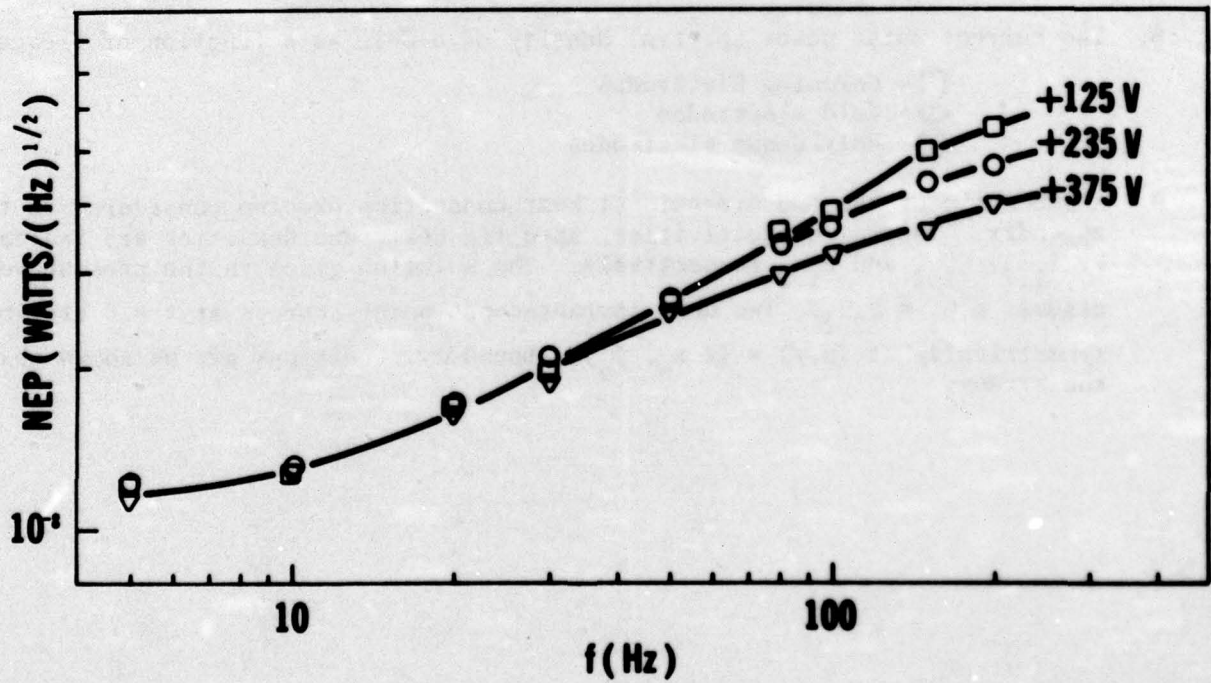


FIG. 2 THE NOISE EQUIVALENT POWER IN THE 8.0 TO 11.5 μm SPECTRAL RANGE

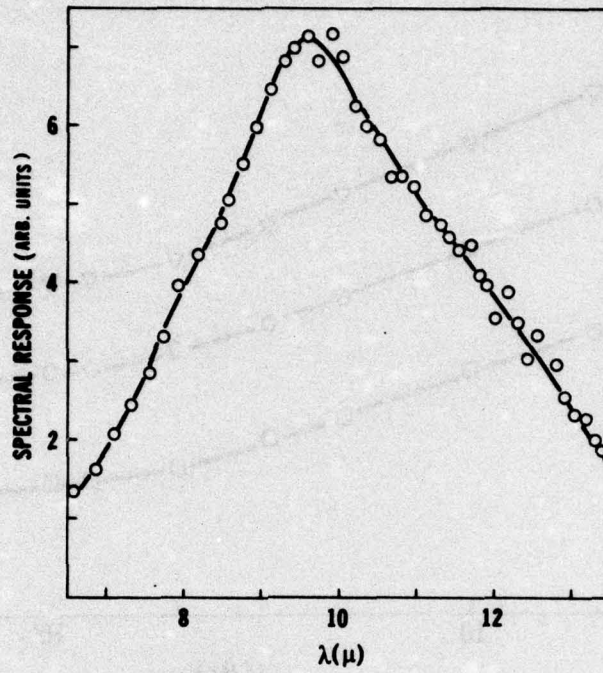


FIG. 3 THE RELATIVE SPECTRAL RESPONSE IN THE 6.5 TO 13.5  $\mu$ m SPECTRAL RANGE

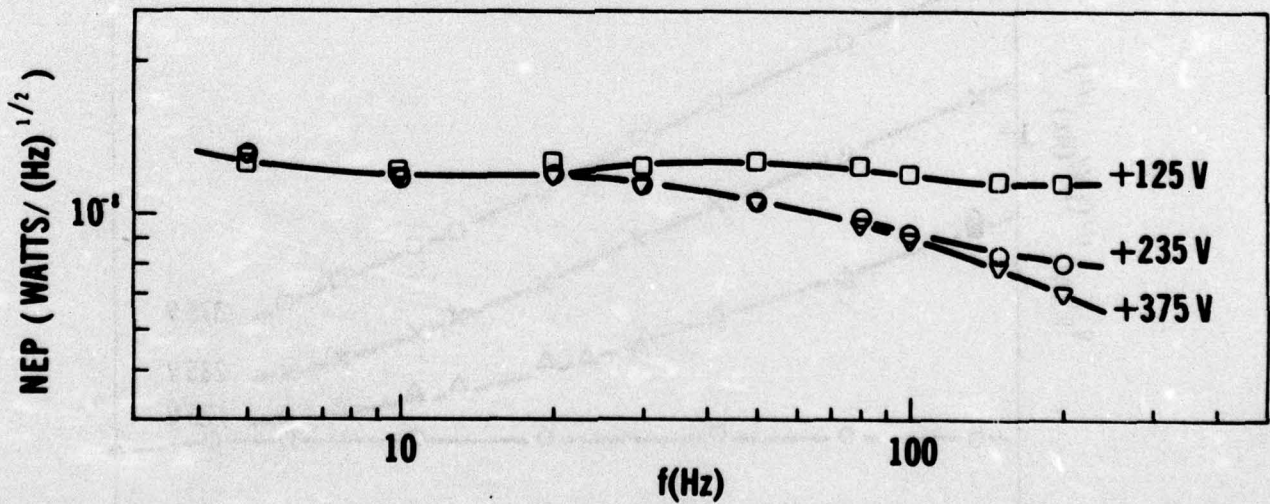


FIG. 4 THE NOISE EQUIVALENT POWER AS A FUNCTION OF FREQUENCY AT  $\lambda=1.1\mu$ m

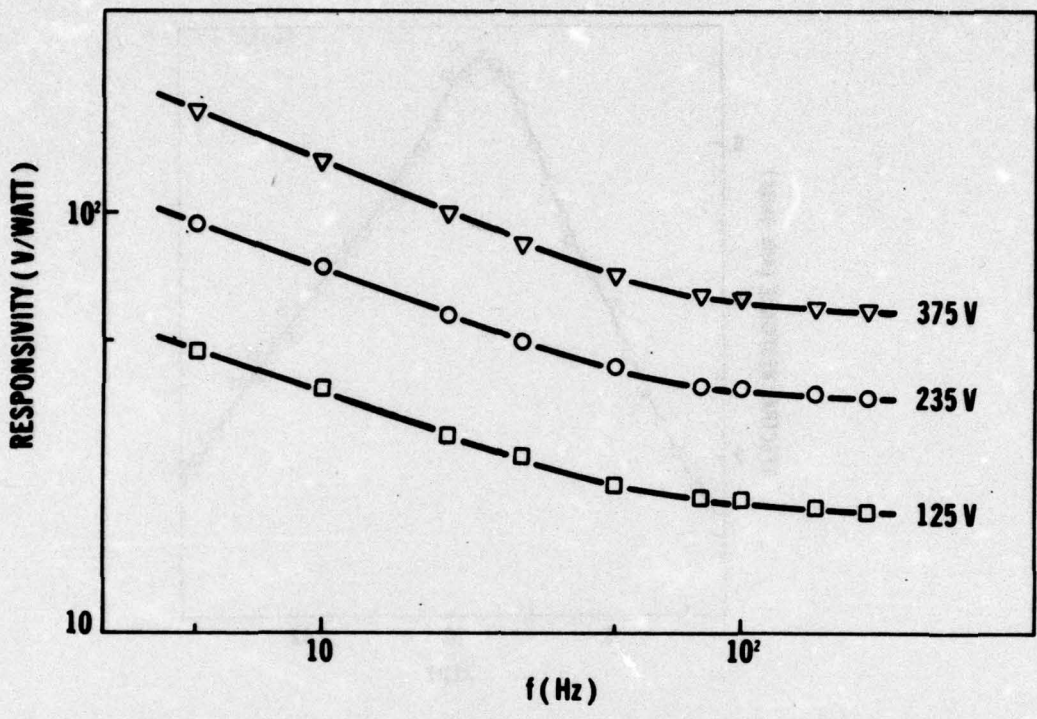


FIG. 5 THE RESPONSIVITY AS A FUNCTION OF FREQUENCY AT  $\lambda=1.1\mu\text{m}$

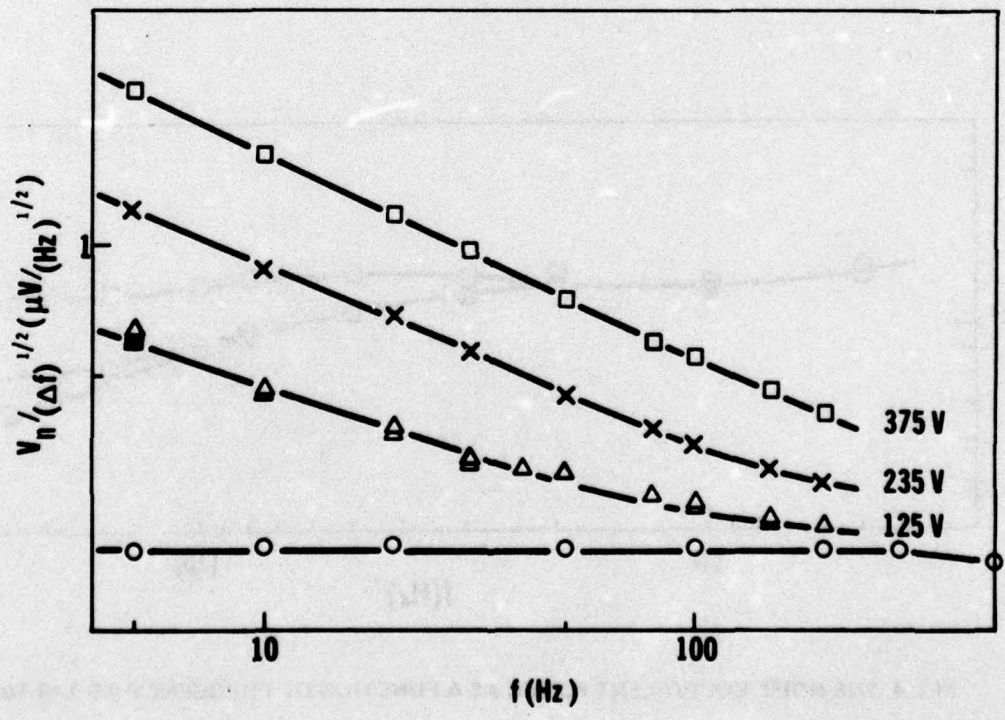


FIG. 6 THE NOISE VOLTAGE AS A FUNCTION OF FREQUENCY

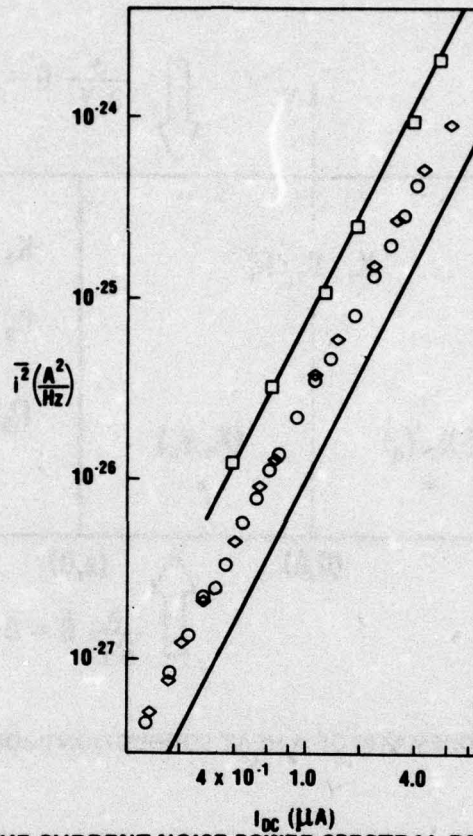


FIG. 7 THE CURRENT NOISE POWER SPECTRAL DENSITY AT  $f=10$  Hz AS A FUNCTION OF APPLIED CURRENT

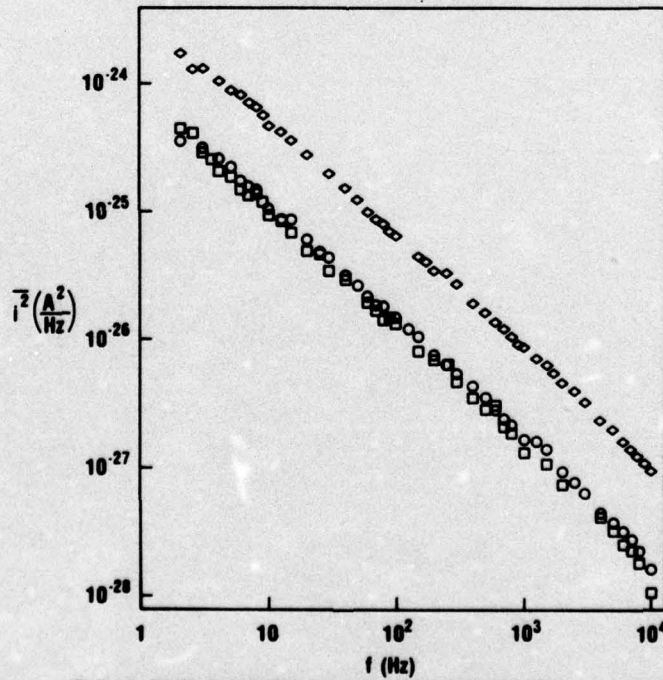


FIG. 8 THE CURRENT NOISE POWER SPECTRAL DENSITY AS A FUNCTION OF FREQUENCY

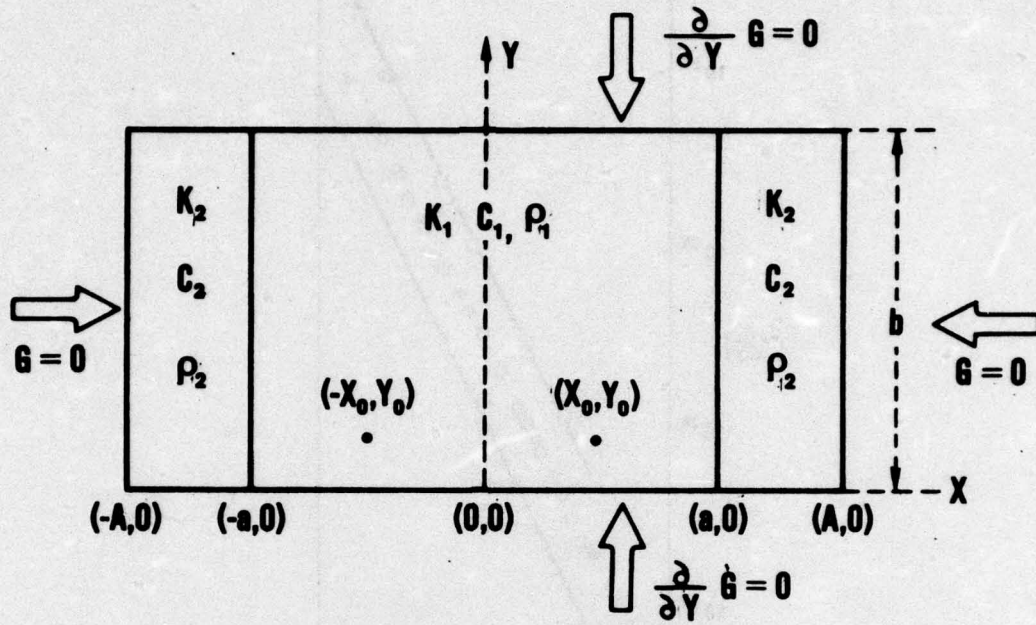


FIG. 9 SCHEMATIC OF A HEAT CONDUCTION PROBLEM

## DISTRIBUTION

|  |                                      |
|--|--------------------------------------|
| Director, Advanced Research Projects Agency<br>1400 Wilson Blvd.<br>Arlington, Va. 22209<br>Attn: Technical Library  | 3                                    |
| Commander, Naval Air Systems Command<br>Washington, D. C. 20360<br>Attn: AIR-310 (Dr. H. J. Mueller)<br>AIR-310B (Dr. J. W. Willis)  | 1<br>1                               |
| Commander, Naval Electronic Systems Command<br>Washington, D. C. 20360<br>Attn: Code 033 (N. Butler)<br>Code 0334 (C. Rigdon)<br>Code 0335 (L. Sumney)<br>Code 034A (R. Fratila)   | 1<br>1<br>1<br>1                     |
| Commander, Naval Sea Systems Command<br>Washington, D. C. 20360<br>Attn: SEA-03B<br>SEA-03416 (S. Barham)<br>SEA-03415 (T. Tasaka)   | 1<br>1<br>1                          |
| Director, Naval Research Laboratory<br>Washington, D. C. 20390<br>Attn: A. Brodzinski, Code 5200<br>J. Davey, Code 5210<br>D. Barbe, Code 5210<br>H. Lessoff, Code 5220<br>J. McCallum, Code 6503<br>R. Greene, Code 5230<br>S. Teitler, Code 6470 | 1<br>1<br>1<br>1<br>1<br>1<br>1<br>1 |
| Office of Naval Research<br>800 North Quincy Street<br>Arlington, Va. 22217<br>Attn: M. Yoder, Code 427<br>L. Cooper, Code 422<br>W. Condell, Code 421<br>D. Ferry, Code 427<br>J. Dimmock, Code 427   | 1<br>1<br>1<br>1<br>1                |
| Director, Defense Documentation Center<br>Cameron Station<br>Alexandria, Virginia 22314  | 12                                   |

Commander, Naval Electronics Laboratory Center  
271 Catalina Blvd.  
San Diego, California 21252  
Attn: H. H. Wieder 1

National Bureau of Standards  
Bldg. 225, Room A-331  
Washington, D. C. 20234  
Attn: Mr. Leedy 1  
Technical Library 1

Commander, Naval Weapons Center  
China Lake, Ca. 93557  
Attn: Mr. Henry Blasic 1  
Technical Library 1

Advisory Group on Electron Devices  
201 Varick Street, 9th Floor  
New York, N. Y. 10014  
Attn: Secretary .3

Naval Explosive Ordnance Disposal Facility  
Indian Head, Md. 20640  
Attn: Technical Library 1

Naval Missile Center  
Point Mugu, Ca. 93010  
Attn: Technical Library (Code 5632.2) 1

Naval Oceanographic Office  
Suitland, Maryland 20373  
Attn: Technical Library (Code 1640) 1

Naval Postgraduate School  
Monterey, Ca. 93940  
Attn: Technical Library (Code 0212) 1

Deputy Chief of Naval Operations (Development) 1  
Technical Analysis and Advisory Group (Code NOP-077D)  
Washington, D. C. 20350